Macedonian Journal of Chemistry and Chemical Engineering, Vol. **41**, No. 1, pp. 37–46 (2022)

MJCCA9 – 846

ISSN 1857-5552
e-ISSN 1857-5625

Received: February 22, 2022
Accepted: March 21, 2022

DOI: 10.20450/mjcce.2022.2490
Original scientific paper

STRUCTURAL AND RAMAN SPECTROSCOPIC CHARACTERIZATION OF TETRAPYRIDINESILVER(I) PERRHENATE, $[Agpy_4]ReO_4$

Vladimir M. Petruševski,[1] Kende Attila Béres,[2,3] Petra Bombicz,[2] Attila Farkas,[4] László Kótai,[2,5] Laura Bereczki[2]

[1]Faculty of Natural Sciences and Mathematics, Ss. Cyril and Methodius University, Skopje, Republic of Macedonia
[2]Research Centre for Natural Sciences, Magyar Tudósok krt. 2., Budapest, H-1117, Hungary
[3]Institute of Chemistry, ELTE Eötvös Loránd University, Pázmány Péter s. 1/A, 1117 Budapest, Hungary
[4]Budapest University of Technology and Economics, Department of Organic Chemistry and Technology, H-1111, Budapest, Műegyetem rkp. 3., Hungary
[5]Deuton-X Ltd, H-2030, Érd, Selmeci u. 89

Tetrapyridinesilver(I) perrhenate $[Agpy_4]ReO_4$ was synthesized, and its crystal structure and Raman spectra were elucidated at low temperatures. The crystal lattice is constructed from isolated tetrahedral cations and anions having no argentophilic interactions. Weak hydrogen bonds are formed between the oxygens of the disordered perrhenate anions and the ortho-hydrogens of the pyridine ligands. No parallel π…π stacking interactions are observed, but C-H…π interactions of the pyridine ligands within columns of cations and between the columns appeared. Correlation analysis for Ag^+, pyridine ligands, and perrhenate ions was performed, and the perrhenate ion and some of the AgN_4 skeleton vibrational modes and pyridine ligand modes in the Raman spectrum of $[Agpy_4]ReO_4$ were assigned.

Keywords: crystal structure; Raman spectra; perrhenates; rhenium compounds; pyridine complexes

СТРУКТУРНА И РАМАНСКА СПЕКТРОСКОПСКА КАРАКТЕРИЗАЦИЈА НА ТЕТРАПИРИДИНСРЕБРО(I) ПЕРРЕНАТ, $[Agpy_4]ReO_4$

Синтетизиран е тетрапиридинсребро(I) перренат $[Agpy_4]ReO_4$. Определена е неговата кристална структура и протолкувани се неговите рамански спектри. Кристалната решетка се состои од изолирани тетраедарски катјони и тетраедарски анјони, кај кои не постојат аргентофилни интеракции. Во структурата постојат слаби водородни врски образувани од несредените кислородни атоми на перренатните анјони и орто-водородите од пиридинските лиганди. Не се регистрирани паралелни π…π „натрупувачки“ интеракции, но постојат C–H…π интеракции од пиридинските лиганди во и помеѓу катјонските „столбови“. Анализата на вибрациите на примитивната ќелија со примена на корелационио метод е спроведена, сметајќи дека во структурата постојат катјони на Ag^+, пиридински лиганди и перренатни јони. Асигнирани се модовите од перренатните јони, како и дел од вибрационите модови на скелетот на AgN_4 и пиридинските лиганди во раманскиот спектар.

Клучни зборови: кристална структура; раманси спектри; перренати; соединенија на рениум; пиридински комплекси

1. INTRODUCTION

An easy way to prepare catalytically active simple or mixed transition metal oxides is a low-temperature thermal treatment of transition metal tetraoxometallate (ClO_4^-, MnO_4^-, SO_4^{2-}, MoO_4^{2-}) complexes with reducing ligands like ammonia[1-5] or pyridine.[6-10] The key factor in the occurrence of the solid-phase quasi-intramolecular redox reactions resulting in these oxide materials is the presence of a hydrogen bond between the N–H or C–H functional groups of the ligand and the M–O moiety of the anion. Although rhenium containing transition metal oxides are important catalysts in various important processes,[11,12] this reaction route has not been studied until now to prepare Re-containing materials. Therefore, in this paper, we present the synthesis, structural characterization, and evaluation of the Raman spectra at low temperatures of compound that has not been extensively studied: tetrapyridinesilver(I) perrhenate, $[Agpy_4]ReO_4$.

2. EXPERIMENTAL

Chemical-grade sodium perrhenate, silver nitrate, and pyridine (Deuton-X Ltd, Hungary, Érd) were used in the synthesis of $[Agpy_4]ReO_4$, which was performed by following a previously published method.[13] The complex was identified by its X-ray powder diffractogram, and chemical analysis (Ag, pyridine, and rhenium content) was performed according to the methods given in.[13]

2.1. *X-ray powder diffraction*

X-ray powder diffraction measurements were performed using a Philips PW-1050 Bragg-Brentano parafocusing goniometer equipped with a Cu anode operated at 40 kV and 35 mA tube power, a secondary beam graphite monochromator, and a proportional counter. Scans were recorded in step mode. Evaluation of the diffraction patterns was performed by full profile fitting techniques.

2.2. *Single-crystal XRD measurement*

Single crystal X-ray diffraction data of $[Agpy_4]ReO_4$ were collected at 138(2) K on a Rigaku RAXIS-RAPID II diffractometer using Mo-$K\alpha$ radiation. Numerical absorption correction[14] was carried out using the program CrystalClear.[15] The SHELX program package under WinGX [16,17] software was applied for the structure solution and refinement. The structure was solved by direct methods. The models were refined by full-matrix least-squares on F^2. Refinement of non-hydrogen atoms was carried out with anisotropic temperature factors. Hydrogen atoms were placed into positions of the expected geometry. Hydrogen atoms were included in the structure factor calculations, but they were not refined. The isotropic displacement parameters of the hydrogen atoms were approximated from the U(eq) value of the atom to which they were bonded. The summary of the data collection and refinement parameters is shown in Table 1. Selected bond lengths and angles of the compounds were calculated by the PLATON software.[18] The graphical representation and the edition of CIF files were done by Mercury[19] and PublCif[20] software packages, respectively. SIMU restraints were applied to the disordered oxygen atoms of the perrhenate anion of $[Agpy_4]ReO_4$. The disordered O1 and O1′ oxygen site occupation factors are 0.6 and 0.4, respectively. The restraints were used to improve the shape of the thermal ellipsoids. CCDC 2154001 contains the supplementary crystallographic data for this paper.

These data can be obtained free of charge from The Cambridge Crystallographic Data Centre via www.ccdc.cam.ac.uk/structures.

2.3. *Raman measurements*

The Raman measurements of $[Agpy_4]ReO_4$ were performed on a Horiba Jobin-Yvon LabRAM-type microspectrometer with an external 532 nm Nd-laser source (~ 40 mW, Olympus BX-40 optical microscope) at 248 K and 123 K (Linkam THMS600 temperature-controlled microscope stage). The laser beam was focused (50× objective), and a D0.6 intensity filter was used to decrease the laser power to avoid thermal degradation of the sample. A confocal hole of 1000 μm and 1800 groove mm^{-1} grating monochromator were used in a confocal system and for light dispersion. The spectral range of 100–4000 cm^{-1} was measured with a 3 cm^{-1} resolution. The exposure time was 7 s.

3. RESULTS AND DISCUSSION

3.1. *Preparation and properties of $[Agpy_4]ReO_4$*

$[Agpy_4]ReO_4$ belongs to the series of $[Agpy_n]XO_4$ (X = Cl, Mn, Re, n = 2, 2.4, 2.5, and 4) pyridinesilver tetraoxometallate complexes.[6-10] Wilke-Dörfurt and Gunzert prepared $[Agpy_4]ReO_4$ in the reaction of silver nitrate with 1 equivalent of perrhenic acid and 10 equivalents of pyridine in a hot solution.[21] Cooling the reaction mixture results in an oil that solidifies quickly, giving crystals with

different habits. The recrystallization from pure pyridine resulted in unstable colorless needle crystals, which were dried in a desiccator containing pyridine vapor. In the absence of pyridine, the compound decomposes quickly and forms a mixture with a pyridine/$AgReO_4$ stoichiometry of ~ 3. $[Agpy_4]ReO_4$ could also be prepared by dissolving silver perrhenate – prepared from $AgNO_3$ and $NaReO_4$[13] – in pyridine, leaving the solution to crystallize in a deep freezer at around –20 °C. Columnar crystals several centimeters long were formed. Single crystals suitable for the diffraction measurement were obtained by cutting. We could not confirm the formation of the $AgReO_4 \cdot 5py$ compound described by Woolf[22] in the solid equilibrium phase in the $AgReO_4$–pyridine system. Instead, the solid equilibrium phase was proved to be $[Agpy_4]ReO_4$.

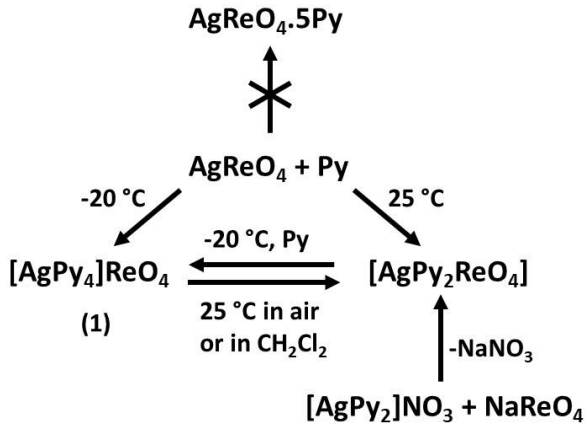

Scheme 1. Preparation routes of $[Agpy_4]ReO_4$

3.2. *Structure of $[Agpy_4]ReO_4$*

Colorless single crystals of $[Agpy_4]ReO_4$ were grown from a pyridine solution of $AgReO_4$ at –20 °C. The crystal data and selected crystallographic parameters of $[Agpy_4]ReO_4$ are listed in Table 1. $[Agpy_4]ReO_4$ crystallizes in the tetragonal crystal system ($I\bar{4}$ space group symmetry). $[Agpy_4]ReO_4$ is isostructural with its analogous perchlorate complex.[23] The lattice constants change slightly, i.e., 12.8045(13)/6.9104(13) Å and 12.874(1)/6.748(4) Å for perrhenate and perchlorate, respectively. The unit cell volume of $[Agpy_4]ReO_4$ is 1.3 % larger than that of $[Agpy_4]ClO_4$. The asymmetric unit of $[Agpy_4]ReO_4$ contains one-quarter of a $[Agpy_4]^+$ cation and one-quarter of a disordered ReO_4^- anion (Fig. 1). O1 and O1′ have a 0.6 : 0.4 occupancy.

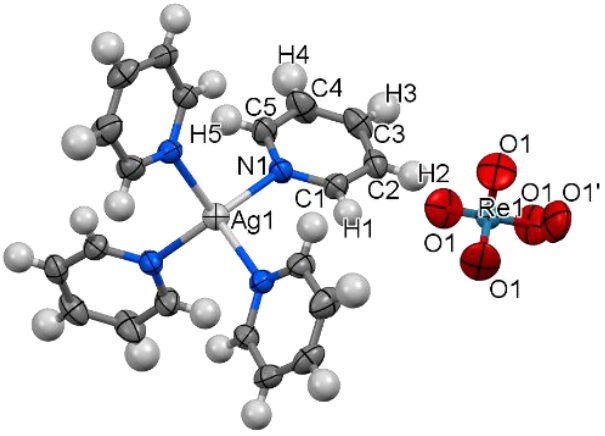

Fig. 1. ORTEP presentation of $[Agpy_4]ReO_4$
(thermal ellipsoids are drawn at the 50 % probability level, hydrogen atoms are omitted for clarity).

T a b l e 1

Crystal data and structure refinement of [Agpy$_4$]ReO$_4$

Empirical formula	$C_{20}H_{20}AgN_4O_4Re$ (**1**)
Formula weight	674.47
Temperature	138(2) K
Radiation and wavelength	Mo-K$_\alpha$, λ = 0.710747 Å
Crystal system	tetragonal
Space group	$I\bar{4}$
Unit cell dimensions	a = 12.8045(13) Å
	b = 12.8045(13) Å
	c = 6.9104(13) Å
	$\alpha = 90°$
	$\beta = 90°$
	$\gamma = 90°$
Volume	1133.0(3) Å^3
Z,Z'	2, 1
Density (calculated)	1.977 Mg/m^3
Absorption coefficient, μ	6.233 mm^{-1}
F(000)	644
Crystal color	colorless
Crystal description	block
Crystal size	0.7 × 0.6 × 0.5 mm
Absorption correction	numerical
Max. and min. transmission	0.056, 0.202
θ – range for data collection	$3.182 \le \theta \le 30.465°$
Index ranges	$-18 \le h \le 18$; $-18 \le k \le 18$; $-9 \le l \le 9$
Reflections collected	14570
Completeness to 2θ	0.998
Absolute structure parameter	0.033(6)
Friedel coverage	0.850
Friedel fraction max.	0.991
Friedel fraction full	0.985
Independent reflections	1713 [*R*(int) = 0.0521]
Reflections $I > 2\sigma(I)$	1713
Refinement method	full-matrix least-squares on F^2
Data / restraints / parameters	1713 /18 /78
Goodness-of-fit on F^2	1.127
Final *R* indices [$I > 2\sigma(I)$]	*R*1 = 0.0193, *wR*2 = 0.0471
R indices (all data)	*R*1 = 0.0193, *wR*2 = 0.0471
Max. and mean shift/esd	0.000;0.000
Largest diff. peak and hole	0.694; –0.693 e.Å^{-3}

The perchlorate ions in the compound [Agpy$_4$]ClO$_4$ are ordered. The [Agpy$_4$]$^+$ cation has a regular tetrahedral geometry. The Ag–N bond distances are 2.308(4) and 2.322(3) Å in the perrhenate and perchlorate complexes, respectively. The N–Ag–N angles are relatively close, i.e., 110.22/107.99° and 112.3/108.1° in the perrhenate and perchlorate complexes, respectively. The Re–O distances are 1.63(2) and 1.74(1) Å. The bond lengths and angles in [Agpy$_4$]ReO$_4$ are listed in Table 2.

T a b l e 2

Selected bond lengths (Å) and angles (°) in [Agpy₄]ReO₄

Re1–O1#1	1.63(2)	Re1–O1#2	1.63(2)
Re1–O1#3	1.63(2)	Re1–O1	1.63(2)
Re1–O1'#1	1.74(1)	Re1–O1'#3	1.74(1)
Re1–O1'#2	1.74(1)	Re1–O1'	1.74(1)
Ag1–N1#4	2.308(4)	Ag1–N1#5	2.308(4)
Ag1–N1#6	2.308(4)	Ag1–N1	2.308(4)
C4–C3	1.38(1)	C4–C5	1.389(8)
N1–C5	1.336(6)	N1–C1	1.343(6)
C3–C2	1.378(9)	C2–C1	1.375(7)
O1#1–Re1–O1#2	125(2)	O1#1–Re1–O1#3	82(4)
O1#2–Re1–O1#3	125(2)	O1#1–Re1–O1	125(2)
O1#2-Re1–O1	82(4)	O1#3–Re1–O1	125(2)
O1#1–Re1–O1'#1	25(1)	O1#2–Re1–O1'#1	112(2)
O1#3–Re1–O1'#1	106(3)	O1–Re1–O1'#1	104(2)
O1#1–Re1–O1'#3	106(3)	O1#2-Re1–O1'#3	104(2)
O1#3–Re1–O1'#3	25(1)	O1–Re1–O1'#3	112(2)
O1#1–Re1–O1'#2	104(2)	O1#2–Re1–O1'#2	25(1)
O1#3–Re1–O1'#2	112(2)	O1–Re1–O1'#2	106(3)
O1'#1–Re1–O1'#2	100.0(9)	O1'#3–Re1–O1'#2	100.0(9)
O1'#1–Re1–O1'	100.0(9)	O1'#3–Re1–O1'	100.0(9)
O1'#2–Re1–O1'	131(2)	N1#4–Ag1–N1#5	108.0(2)
N1#4–Ag1–N1#6	110.2(1)	N1#5–Ag1–N1#6	110.2(1)
N1#4–Ag1–N1	110.2(1)	N1#5-Ag1-N1	110.2(1)
N1#6-Ag1–N1	108.0(2)	C3–C4–C5	118.9(5)
C5–N1–C1	117.5(4)	C5–N1–Ag1	121.7(3)
C1–N1–Ag1	120.6(3)	C4–C3–C2	119.0(5)
N1–C5–C4	122.6(5)	C1–C2–C3	118.6(5)
N1–C1–C2	123.4(5)		

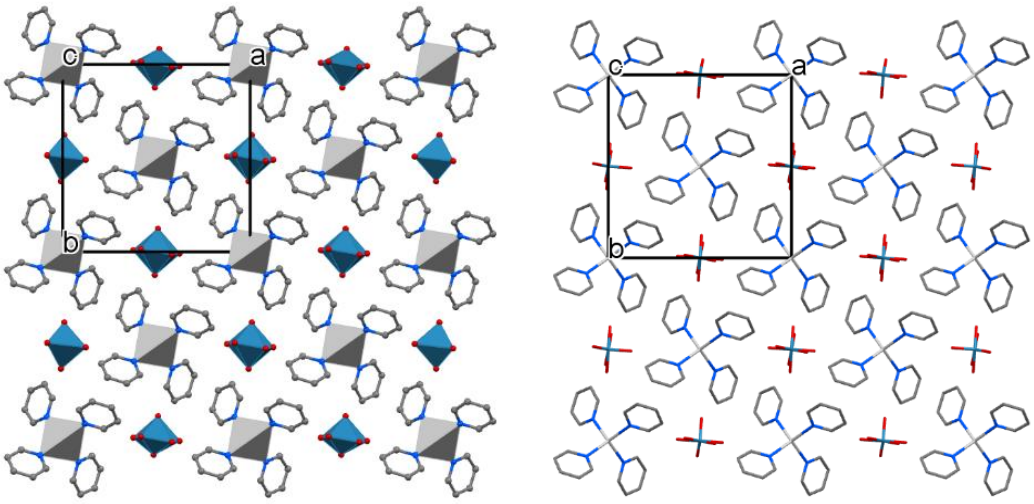

Fig. 2. Packing diagram of [Agpy₄]ReO₄
(View from the *c* axis direction, left: polyhedral coordination presentation; right: stick presentation)

Both the cations and anion of [Agpy₄]ReO₄ are sitting on two-fold axes and four-fold rotoinversion axes (Fig. 2). Weak hydrogen bonds are formed between the disordered O1 and O1′ oxygens of the perrhenate anion and the H1 ortho-hydrogen of the pyridine ligand (Fig. 3, Table 3).

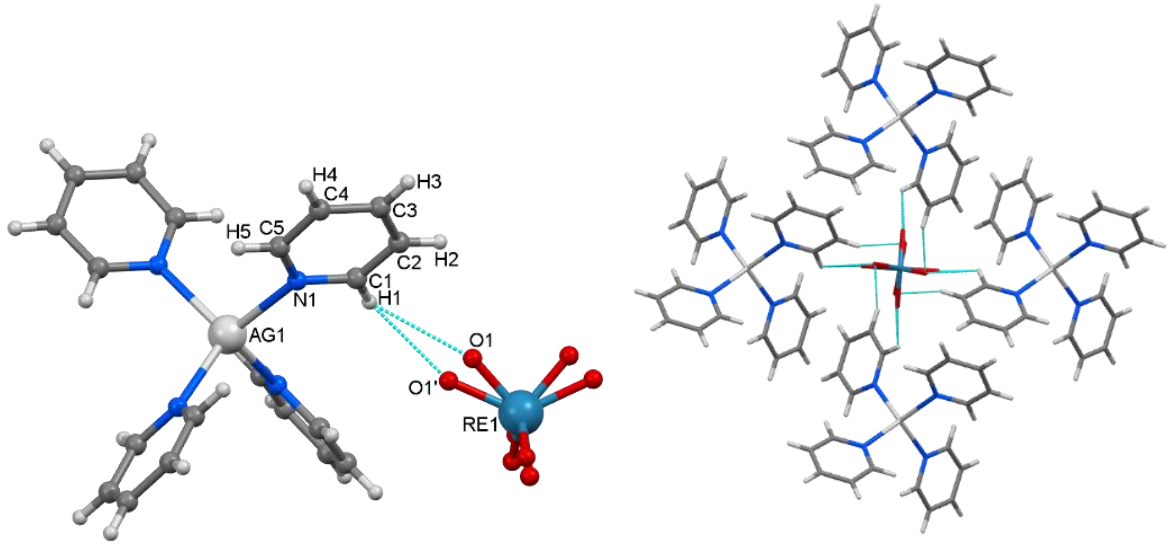

Fig. 3. Hydrogen bonds in the structure of $[Agpy_4]ReO_4$ (hydrogen bonds are marked by cyan dashed lines)

T a b l e 3

Analysis of potential hydrogen bonds and schemes with d(D···A) < R(D)+R(A)+0.50, d(H···A) < R(H)+R(A)-0.12 Å, D-H···A > 100.0° (R: Van der Waals (or ion) radii used in the analysis).

Donor – H...Acceptor	Symm. op.	D – H	H...A	D...A	D – H...A
C1--H1..O1'	–1+*y*,1–*x*,1–*z*	0.93	2.45	3.16(3)	133
C1--H1..O1	–1+*y*,1–*x*,1–*z*	0.93	2.57	3.18(4)	124

The shortest H···O distances (2.45 and 2.57 Å) in $[Agpy_4]ReO_4$ are shorter than in the corresponding perchlorate ($[Agpy_4]ClO_4$, 2.712 Å).[23] No parallel π···π stacking interactions are formed in the structure. C–H···π interactions of the pyridine ligands are formed within columns of cations and between the columns as well. Aromatic interactions are summarized in Table 4.

In $[Agpy_4]ReO_4$, the perrhenate anions are placed in the crystal lattice separately, and the space occupied by the anions is 17.9% (Fig. 4).

T a b l e 4

Analysis of short ring-interactions in $[Agpy_4]ReO_4$ indicating Cg–Cg distances < 6.0 Å, α < 20° and β < 60°

Cg(I) Res(I) Cg(J)	Symm. op.	Cg–Cg [Å]	α [°]	β [°]	γ [°]	CgI_Perp [Å]	CgJ_Perp [Å]
Cg1 [1] -> Cg1	1–*x*, 1–*y*, *z*	5.856(3)	82.0(3)	54.8	54.8	3.374(2)	3.374(2)
Cg1 [1] -> Cg1	1–*y*, *x*, –*z*	4.795(3)	64.5(3)	11.4	67.3	1.847(2)	4.700(2)
Cg1 [1] -> Cg1	1/2–*x*, 3/2–*y*, 1/2+*z*	4.918(3)	82.0(3)	8.2	86.1	0.333(2)	4.868(2)

(α = Dihedral angle between planes I and J (°); β = Angle Cg(I)→Cg(J) or Cg(I)→Me vector and normal to plane I (°); γ = Angle Cg(I)→Cg(J) vector and normal to plane J (°); Cg–Cg = Distance between ring centroids (Å); CgI_Perp = Perpendicular distance of Cg(I) on ring J (Å); CgJ_Perp = Perpendicular distance of Cg(J) on ring I (Å).

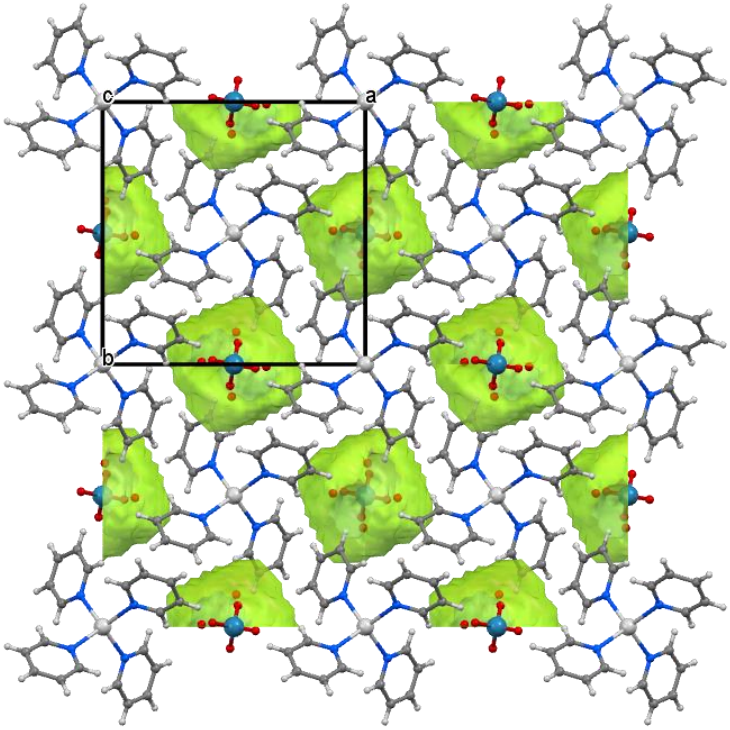

Fig. 4. Arrangement of perrhenate anions in the crystal lattice

3.3. *Correlation analysis and low-temperature Raman spectra of [Agpy₄]ReO₄*

The primitive cell of $[Agpy_4]ReO_4$ (Z = 1) contains 50 atoms, equivalent to 150 degrees of freedom. The correlation table for the ReO_4^- anions at S_4 sites in $[Agpy_4]ReO_4$ (Fig. 5) shows 9 internal vibrational modes. The B and E modes are IR and Raman active, whereas the A modes are only Raman active. The E modes are doubly degenerate. Accordingly, bands 5 and 7 due to internal vibrations are expected in the IR and the Raman spectra, respectively. The Ag^+ site is the same as for perrhenate; thus, the same correlations can be expected for the AgN_4 skeleton as well. For the external vibrations of the ReO_4^- anions at S_4 sites, a total of 6 vibrational degrees of freedom (3 of translational and 3 of rotational origin) are expected. The corresponding bands are expected in the far IR region (5 bands) and in the low-frequency part of the Raman spectra (6 bands). *R* and *T* denote hindered rotations and hindered translations of the anions, respectively. No predictions of the intensities can be given *a priori*.

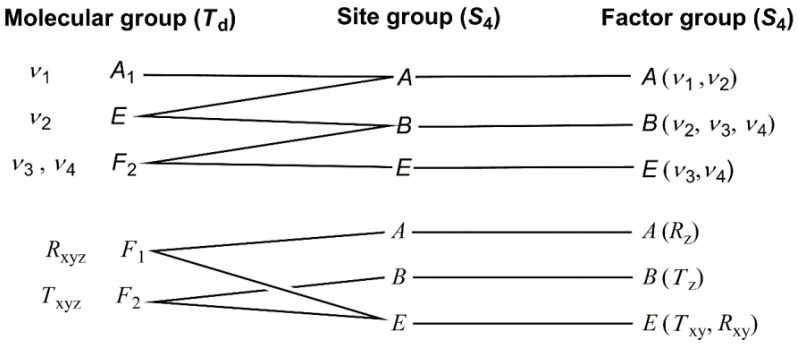

Fig. 5. Correlation table for perrhenate ions in $[Agpy_4]ReO_4$

The hindered translations of Ag^+ cations at S_4 sites show a total of 3 vibrational degrees of freedom (one Ag^+ ion per primitive cell). The two hindered translations are both Raman and IR active (Fig. 6).

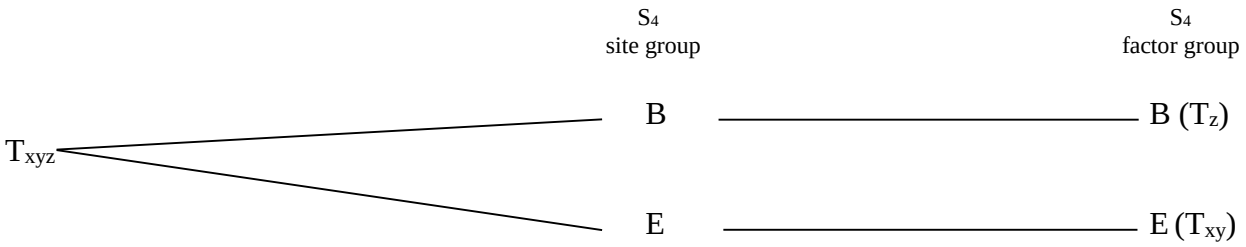

Fig. 6. Correlation table for the silver ion in [Agpy$_4$]ReO$_4$

The correlation table shows the 27 internal vibrational modes of the pyridine rings at C_1 sites. Each mode from the local (site) group splits into 3 components in the factor group. There are 27 A, 27 B, and 27 E modes, giving rise to 108 vibrational degrees of freedom. All factor group modes are Raman active, while only the B and E modes are IR active. The number of factor group modes due to internal vibrations is 108, as it should be for 4 pyridine molecules. The external vibrational modes of one type of pyridine rings at C_1 sites are shown in Figure 7. Each mode from the local (site) group splits into 3 components in the factor group. There are 6 A, 6 B, and 6 E modes, giving rise to a total of 24 vibrational degrees of freedom. There are 12 degrees of freedom for hindered translations and 12 for hindered rotations.

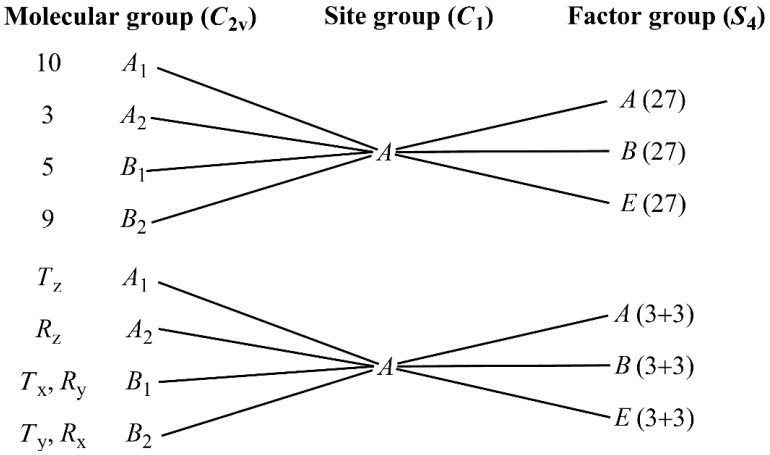

Fig. 7. Correlation table for the coordinated pyridine molecules in [Agpy$_4$]ReO$_4$

Of the above modes (i.e., 36A, 38 B, and 38 E modes), 1B and 1 E are acoustic modes. The latter modes, under the **k** = 0 approximation, are of 0 frequency. One would, therefore, expect at most 36 A, 37 B, and 37 E bands due to fundamental transitions to appear in the Raman (110) and the IR (74) spectra. The bands due to second-order transitions, as always, can, in principle, further complicate the spectral picture.

3.4. *Low-temperature Raman spectra of [Agpy$_4$]ReO$_4$*

[Agpy$_4$]ReO$_4$ easily decomposes at room temperature; thus, neither IR nor Raman measurements could be done without in-situ contamination of [Agpy$_4$]ReO$_4$ during the measurement with other pyridine-containing complexes (Scheme 1). In order to study the AgN_4 skeleton and perrhenate vibrational modes, low-temperature (248 K and 113 K) Raman measurements were performed (Fig. 8).

All four vibrational modes (symmetric and antisymmetric stretching (ν_1 or ν_s and ν_3 or ν_{as}) and bending (ν_2 or δ_s and ν_4 or δ_{as}), respectively) of the tetrahedral AgN_4 skeleton and perrhenate ions are Raman active. The regular T_4 geometry of the AgN_4 skeleton on the S4 site gave the same Ag-N modes as the perrhenate ion; thus, 7 Raman active bands can be expected.

The Raman spectra recorded at 253 and 113 K are shown in the ESI (Electronic Supplementary Information) Figures 1–3 and Figure 8.

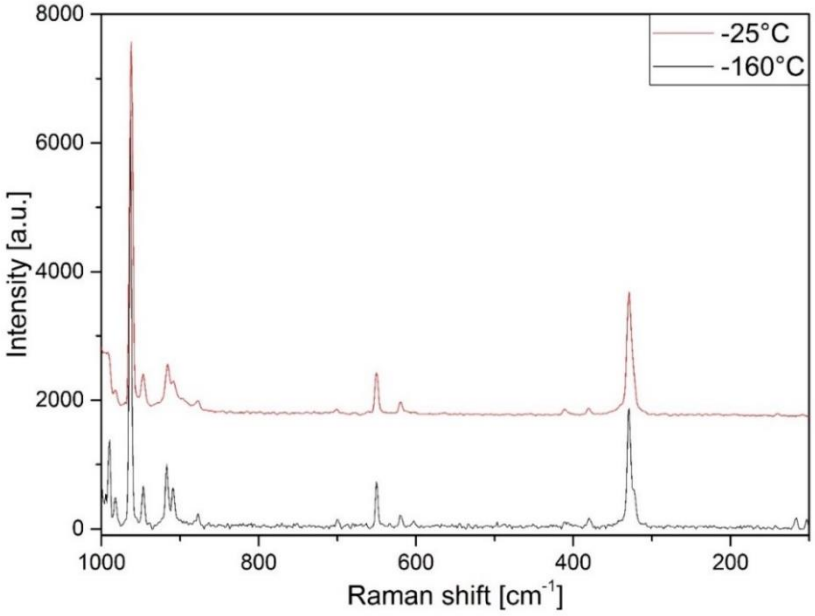

Fig. 8. Raman spectra of $[Agpy_4]ReO_4$ at 113 K and 248 K in the 1000–100 cm^{-1} range

The singlet $\nu_s(A_1)$ mode can easily be assigned at 964 cm^{-1} as a relatively intense peak in the Raman spectrum of $[Agpy_4]ReO_4$ measured at 113 K. The weak doublet (A+E) of ν_{as}(Re–O) can be seen at 907 and 919 cm^{-1}. No splitting of δ_s and δ_{as} modes (329 and 349 cm^{-1}, respectively) could be observed. The ν_s (Ag–N) mode assigned by Bowmaker at 88 cm^{-1} for the $[Agpy_4]^+$ ion and the ν_T modes[24] around 65–73 cm^{-1} are out of our measurement range. Bowmaker[24] found a band in the spectra of $4[Agpy_2ClO_4]\cdot[Agpy_4]ClO_4$ around 100 cm^{-1}, which was attributed to the Ag–O contribution of the coordinated perchlorate ion. A weak band was observed in the Raman spectrum of $[Agpy_4]ReO_4$ as well; however, due to the lack of the coordinated perrhenate, the Ag–O bond may not contribute to the band observed around ~100 cm^{-1}. Therefore, this peak may belong to ν_s(Ag–N).

The very weak Raman band belonging to the ν_{as}(Ag–N) mode of the $[Agpy_4]^+$ cation in the Raman spectrum of $4[Agpy_2MnO_4]\cdot[Agpy_4]MnO_4$ was found at 124 cm^{-1}.[8] For the studied compound, this mode in the Raman spectrum was attributed to the band at 118 cm^{-1}. A lattice mode belonging to the perrhenate ion was observed at 144 cm^{-1},[25] whereas lattice modes related to the cationic part[25] were assigned between 190 and 160 cm^{-1}. Some characteristic pyridine ring vibrational modes were also found, the most intense band being prescribed to the C–H wag mode of the pyridine ring at 1072 cm^{-1}. The rest of the assigned pyridine ring modes are summarized in ESI Table 1.

4. CONCLUSION

The structure of tetrapyridinesilver(I) perrhenate $[Agpy_4]ReO_4$ contains isolated tetrahedral cations and anions without argentophilic interactions. Weak hydrogen bonds are formed between the oxygens of the disordered perrhenate anions and the ortho-hydrogens of the pyridine ligands. No parallel π…π stacking, but there are C–H···π interactions of the pyridine ligands within and between the columns of the cations. The low-temperature Raman spectroscopic studies and correlation analysis resulted in the assignation of perrhenate and some of the AgN_4 skeleton vibrational modes of $[Agpy_4]ReO_4$.

Acknowledgment: The research was supported by the European Union and the State of Hungary, co-financed by the European Regional Development Fund (VEKOP-2.3.2-16-2017-00013) (LK) and the ÚNKP-21-3 New National Excellence Program of the Ministry for Innovation and Technology from the source of the National Research, Development and Innovation Fund (KAB). The authors thank the National Research, Development and Innovation Office (OTKA 124544).

REFERENCES

(1) Fogaca, L. A.; Kováts, É.; Németh, G.; Kamarás, K.; Béres, K. A.; Németh, P.; Petruševski, V.; Bereczki, L.; Holló, B. B.; Sajó, I. E., Solid-phase quasi-intramolecular redox reaction of $[Ag(NH_3)_2]MnO_4$: an easy way to prepare pure $AgMnO_2$, *Inorg. Chem.* **2021**, *60* (6), 3749–3760. https://doi.org/10.1021/acs.inorgchem.0c03498.

(2) Solt, H. E.; Németh, P.; Mohai, M.; Sajó, I. E.; Klébert, Sz.; Franguelli, F. P.; Fogaca, L. A.; Pawar, R. P.; Kótai, L., Temperature-limited synthesis of copper manganites along the borderline of the amorphous/crystalline state

and their catalytic activity in CO oxidation, *ACS Omega* **2021**, *6* (2), 1523–1533. http://doi.org/10.1021/acsomega.0c05301.

(3) Fogaca, L. A.; Bereczki, L.; Petruševski, V. M.; Holló, B. B.; Franguelli, F. P.; Mohai, M.; Béres, K. A.; Sajó, I. E.; Szilágyi, I. M.; Kotai, L., A Quasi-intramolecular solid-phase redox reaction of ammonia ligands and perchlorate anion in diamminesilver(I) perchlorate, *Inorganics* **2021**, *9* (5), 38–57 (2021). https://doi.org/10.3390/inorganics9050038.

(4) Franguelli, F. P.; Holló, B. B.; Petruševski, V. M.; Sajó, I. E.; Klébert, Sz.; Farkas, A.; Bódis, E.; Szilágyi, I. M.; Pawar, R. P.; Kótai, L., Thermal decomposition and spectral characterization of di[carbonatotetraamminecobalt(III)] sulfate trihydrate and the nature of its thermal decomposition products, *J. Therm. Anal. Calorim.* **2021**, *145* (9), 2907–2923. https://doi.org/10.1007/s10973-020-09991-3.

(5) Béres, K. A.; Sajó, I. E.; Lendvay, Gy.; Trif, L.; Petruševski, V. M.; Holló, B. B.; Korecz, L.; Franguelli, F. P.; Szilágyi, I. M.; Kótai, L., Solid-phase "self-hydrolysis" of $[Zn(NH_3)_4MoO_4@2H_2O]$ involving enclathrated water — An easy route to a layered basic ammonium zinc molybdate coordination polymer, *Molecules* **2021**, *26* (13), 4022–4041. https://doi.org/10.3390/molecules26134022.

(6) Franguelli, F. P.; Béres, K. A.; Kótai, L., Pyridinesilver tetraoxometallate complexes: overview of the synthesis, structure, and properties of pyridine complexed $AgXO_4$ (X = Cl, Mn, Re) compounds, *Inorganics* **2021**, *9* (11), 79–92. https://doi.org/10.3390/inorganics9110079.

(7) Holló, B. B.; Petruševski, V. M.; Kovács, G. B.; Franguelli, F. P.; Farkas, A.; Menyhárd, A.; Lendvay, Gy.; Sajó, I. E.; Bereczki, L.; Pawar, R. P.; Szilágyi, I. M.; Bódis, E.; Kótai, L., Thermal and spectroscopic studies on a double-salt-type pyridine–silver perchlorate complex having κ_1-O coordinated perchlorate ions, *J. Therm. Anal. Calorim.* **2019**, *138* (2), 1193–1205. https://doi.org/10.1007/s10973-019-08663-1.

(8) Kovács, G. B.; May, N. V.; Bombicz, P. A.; Klébert, Sz.; Németh, P.; Menyhárd, A.; Novodárszki, Gy.; Petruševski, V.; Franguelli, F. P.; Magyari, J.; Béres, K.; Szilágyi, I. M.; Kótai, L., An unknown component of a selective and mild oxidant: structure and oxidative ability of a double salt-type complex having κ_1O-coordinated permanganate anions and three- and four-fold coordinated silver cations, *RSC Adv.* **2019**, *9* (49), 28387–28398. https://doi.org/10.1039/C9RA03230D.

(9) Kótai, L.; Fodor, J.; Jakab, E.; Sajó, I. E.; Szabó, P.; Lónyi, F.; Valyon, J.; Gács, I.; Argay, Gy.; Banerji, K. K., A thermally induced low-temperature intramolecular redox reaction of bis(pyridine)silver(I) permanganate and its hemipyridine solvate, *Transit. Met. Chem.* **2006**, *31* (1), 30–34. https://doi.org/10.1007/s11243-005-6322-2.

(10) Kótai, L.; Sajó, I. E.; Fodor, J.; Szabó, P.; Jakab, E.; Argay, G.; Holly, S.; Banerji, K. K., Reasons for and consequences of the mysterious behavior of newly prepared hemipyridine solvate of bis(pyridine)silver(I) permanganate, $Agpy_2MnO_4$*0.5py, *Transit. Met. Chem*. **2005**, *30* (8), 939–943. https://doi.org/10.1007/s11243-005-6231-4.

(11) Salaev, M. A.; Salaeva, A. A.; Vodyankina, O. V., Towards the understanding of promoting effects of Re, Cs and Cl promoters for silver catalysts of ethylene epoxidation: A computational study, *Catalysis Today* **2021**, *375*, 585–590. https://doi.org/10.1016/j.cattod.2020.04.057.

(12) Ren, D.; Cheng, G.; Li, J.; Li, J.; Dai, W.; Sun, X. X.; Cheng, D., Effect of rhenium loading sequence on selectivity of Ag–Cs catalyst for ethylene epoxidation, *Catalysis Letters* **2017**, *147*, 2920–2928. https://doi.org/10.1007/s10562-017-2211-5.

(13) Sajó, I. E.; Kovács, G. B.; Pasinszki, T.; Bombicz, P. A.; May, Z.; Szilágyi, I. M.; Jánosity, A.; Banerji, K. K.; Kant, R.; Kótai, L., The chemical identity of "[Ag-py_2]MnO_4" organic solvent-soluble oxidizing agent and new synthetic routes for the preparation of $[Agpyn]XO_4$ (X = Mn, Cl, and Re, n = 2-4) complexes, *J. Coord. Chem*. **2018**, *71* (16-18), 2884–2904. DOI: https://doi.org/10.1080/00958972.2018.1493464.

(14) Higashi, T., *Numerical Absorption Correction*, NUMABS, 2002.

(15) CrystalClear SM 1.4.0 Rigaku/MSC Inc., 2008.

(16) Sheldrick, G. M., Crystal structure refinement with *SHELXL*, Program for Crystal Structure Refinement, University of Göttingen, Germany, *Acta Cryst.* **2015**, *C71* (1), 3–8. https://doi.org/10.1107/S2053229614024218.

(17) Farrugia, L. J., WinGX and ORTEP for Windows: an update, *J. Appl. Crystallogr*. **2012**, *45* (4), 849–854. https://doi.org/10.1107/S0021889812029111.

(18) Spek, A. L., Single crystal structure validation with the program PLATON, *J. Appl. Cryst.* **2003**, *36* (1) 7–13. https://doi.org/10.1107/S0021889802022112.

(19) Macrae, C. F.; Edgington, P. R.; McCabe, P.; Pidcock, E.; Shields, G. P.; Taylor, R.; Towler, M.; Van de Streek, J., Mercury: visualization and analysis of crystal structures, *J. Appl. Cryst.* **2006**, *39* (3), 453–457. https://doi.org/10.1107/S002188980600731X.

(20) Westrip, S. P., publCIF: software for editing, validating and formatting crystallographic information files, *J. Appl. Crystallog*. **2010**, *43* (4), 920–925. https://doi.org/10.1107/S0021889810022120.

(21) Wilke-Dörfurt, E.; Gunzert, Th., Über neue Salze der Perrheniumsäure, *Z. Anorg. Allgem. Chem.* **1933**, *215* (3–4), 369–387. https://doi.org/10.1002/zaac.19332150316.

(22) Woolf, A. A., A comparison of silver perrhenate with silver perchlorate, *J. Less-Common Metals.* **1978**, *61* (1), 151–160. https://doi.org/10.1016/0022-5088(78)90154-6.

(23) Nilsson, K.; Oskarsson, A., The crystal structure of tetrapyridinecopper(I) perchlorate and tetrapyridinesilver(I) perchlorate at 260 K, *Acta Chem. Scand.* **1982**, *A36* (7), 605–610. DOI: 10.3891/acta.chem.scand.36a-0605.

(24) Bowmaker, G. A.; Effendy; Lim, K. C.; Skelton, B. W.; Sukarianingsih, D.; White, A. H., Syntheses, structures and vibrational spectroscopy of some 1:2 and 1:3 adducts of silver(I) oxyanion salts with pyridine and piperidine bases containing non-coordinating 2(,6)-substituents, *Inorg. Chim: Acta* **2005**, *358* (14), 4342–4370. https://doi.org/10.1016/j.ica.2005.04.008.

(25) Gassman, P. L.; McCloy, J. S.; Soderquista, C. Z.; Schweiger, M. J., Raman analysis of perrhenate and pertechnetate in alkali salts and borosilicate glasses, *J. Raman Spectr*. **2014**, *45* (1), 139–147. DOI: 10.1002/jrs.4427.